

Energy-Efficient Aerial Network Slicing for Computation Offloading, Data Gathering, and Content Delivery

Ahmed A. Al-habob, Senior Member, IEEE, Octavia A.

Dobre, Fellow, IEEE, and Yindi Jing, Senior Member, IEEE

Abstract

This paper introduces an unmanned aerial vehicle (UAV)-enabled network slicing problem to provide content delivery, sensing data gathering, and mobile edge computing (MEC) services. Three tenants provide services to their clients by sharing a common infrastructure of a set of UAVs. The content delivery tenant needs to guarantee that each of its clients (users) receives the required content, the sensing tenant aims to gather an adequate amount of uncorrelated data, and the MEC tenant provides computing service to its clients. An energy consumption minimization framework is considered to meet the tenants' requirements by optimizing the number of deployed UAVs, the deployment location of each UAV, the transmit power of each deployed UAV, the user-UAV association, and the transmission power as well as the computing resources of each UAV. Taking into account the spatial correlation among the sensing users, a subset of these users is activated to gather the required sensing information. A solution approach technique inherited from graph theory is presented, in which the Lagrange approach derives the transmission power and computing resource allocation expressions. Simulation results illustrate that the proposed framework significantly reduces the total energy consumption.

Index Terms

Content delivery, mobile edge computing, network slicing, spatially-correlated data gathering, unmanned aerial vehicle (UAV).

I. Introduction

The recent development of communication networks, such as the fifth generation (5G) and beyond 5G networks, is associated with a major development in the networks' infrastructure

and resources [1]. Alongside the growth of communication networks, smartphone devices and vehicular systems exhibit more computing and sensing capabilities, which increases the amount and diversity of the gathered data. The sensing capability of devices has given birth to an emerging paradigm, namely mobile crowd sensing (MCS), which enables devices to build participatory sensor networks [2]. The MCS devices can collect sufficient information regarding the detection of physical phenomena or surrounding conditions such as traffic or temperature. By designing appropriate rewards for the contributed devices, the participation of the devices can be decided. The reward of each contributing device can be proportional to the importance or novelty of the data obtained by the device. Some work in the literature has investigated the aggregation of data from a group of devices considering the spatial correlation [3], [4] and/or the novelty of information [5].

Content delivery represents an important aspect of the 5G networks as daily generated content (e.g., YouTube videos, Dropbox shared files, Instagram pictures) witness exponential growth in their quality and quantity requirements. Multiple efforts have been devoted to developing different techniques for content delivery, such as network coding [6] and unmanned aerial vehicle (UAV)-enabled data delivery scenarios [7], [8]. The evolution of 5G networks is associated with increased computing capabilities throughout these networks, especially at the edges, which gives birth to the mobile-edge computing (MEC) paradigm to provide task offloading services in terrestrial and non-terrestrial networks [9]. Integrating aerial devices (such as UAVs and high-altitude platforms) into 5G networks enables flexible and cost-efficient infrastructure deployment as well as providing services, including MEC services, in areas lacking ground infrastructure [10]–[12]. UAV-enabled networks leverage the line-of-sight (LoS) dominant UAV-ground communication channels, which can also include non-LoS (NLoS) links in some locations with different characteristics, such as urban areas [13].

Network slicing enables the coexistence of multiple virtual networks that share the same infrastructure while providing different services with heterogeneous requirements [14]. Network slicing enables mobile network operators to lease their communications resources, such as base stations, cell sites, and data centers, to service providers or tenants which offer services to their customers or users [15]. The tenants lease resource slices to meet their customers demands while the network operators provide the resources [16]. This concept is referred to as network-as-a-service (NaaS), which makes optimal allocation of the available

communication infrastructure and resources a critical challenge that must be addressed to meet the tenants' obligation and benefit the operators.

TABLE I
Main Notations Used in the Paper.

Notation	Description	Notation	Description
N	Total number of users in the users set \mathcal{N}	U	Number of available UAVs in the UAVs set \mathcal{U}
$\mathcal{N}_c/\mathcal{N}_s/\mathcal{N}_m$	Set of content delivery/sensing/MEC users, $\mathcal{N} = \{\mathcal{N}_c, \mathcal{N}_s, \mathcal{N}_m\}$	K	Number of deployed UAVs $K \leq U$
$N_c/N_s/N_m$	Number of content delivery/sensing/MEC users, $N = N_c + N_s + N_m$	C	Number of contents in the content catalog \mathcal{C}
$n_i/u_k/c_j$	User n_i / UAV u_k / content item c_j	M_j	Size of content c_j (in bits)
$\mathbf{R} = [r_{ij}]_{N_c \times C}$	Content demand indicator, r_{ij} is defined in (1)	$\mathbf{S} = [s_{jk}]_{C \times U}$	UAVs' content storage indicator, s_{jk} is defined in (2)
L	Size of the raw data gathered by a sensing user	H	Size of the uncorrelated data (information) of all sensing users
$\boldsymbol{\eta} = [\eta_i]_{N_s \times 1}$	Sensing users activation decision variable, η_i is defined in (5)	$\mathcal{H}(\boldsymbol{\eta})$	Size of information of the active sensing users
ρ	Data correlation extent parameter	ℓ_i/ς_i	Task size/number of CPU cycles to compute one bit of user $n_i \in \mathcal{N}_m$
\mathbf{h}_{ik}	Communication channel vector between a user n_i and a UAV u_k	$\psi_k = \{x_k, y_k, z_k\}$	Cartesian coordinates of the placement location of u_k
$d_{ik} = \ \psi_k - \tilde{\psi}_i\ $	Distance between the user n_i and UAV u_k	$\tilde{\psi}_i = \{\bar{x}_i, \bar{y}_i, 0\}$	Cartesian coordinates of user n_i
λ_0	Path loss at the reference distance of 1 meter	β/F	Path loss exponent/Rician factor
$P_k/F_k/A_k$	Transmit power/computing speed/number of antennas of UAV u_k	$\mathbf{h}_{ik}^{\text{LoS}}/\mathbf{h}_{ik}^{\text{NLoS}}$	LoS/NLoS components of the channel \mathbf{h}_{ik}
ϕ_{ik}	Angle between user n_i and UAV u_k	$\boldsymbol{\mu} = [\mu_{ik}]_{N \times U}$	User-UAV association decision variable, μ_{ik} is defined in (9)
P_{ik}	The allocated transmit power for user n_i at UAV u_k	$\mathbf{w}_{ik}T$	Beamformer for user n_i at UAV u_k
$\mathbf{P} \triangleq [p_1, \dots, p_K]$	Power allocation decision with $\mathbf{p}_k = [P_{1k}, \dots, P_{Nk}]^T$	$\gamma_{ik}(\boldsymbol{\eta}, \boldsymbol{\mu}, \psi)$	Signal-to-interference-plus-noise ratio at user n_i from UAV u_k
$\mathcal{R}_{ik}(\boldsymbol{\eta}, \boldsymbol{\mu}, \psi)$	Data rate at user n_i from UAV u_k	$\tilde{\gamma}_{ik}(\boldsymbol{\eta}, \boldsymbol{\mu}, \psi)$	Signal-to-interference-plus-noise ratio at UAV u_k from user n_i
$\bar{\mathcal{R}}_{ik}(\boldsymbol{\eta}, \boldsymbol{\mu}, \psi)$	Data rate at UAV u_k from user n_i	V	Travelling speed of the UAV
$P^{(\text{prof})}/P^{(\text{ind})}$	Blade profile/induced power of the UAV in hovering status	ϖ	Rotor blade's tip speed
v_0	Hovering mean rotor-induced velocity	δ_0/ζ	Fuselage drag ratio/rotor solidity
ς/ξ	Air density/rotor disc area	$P^{(\text{hov})}$	Hovering power of the UAV
ψ_k^0	Docking location of UAV u_k	$\mathcal{E}_k^{\text{hov}}(\psi)$	Energy consumption of moving UAV u_k from ψ_k^0 to ψ_k
$\mathcal{E}_k^{\text{hov}}(\boldsymbol{\eta}, \boldsymbol{\mu}, \psi, \mathbf{f}, \mathbf{P})$	Energy consumption of UAV u_k while hovering at ψ_k	$\mathcal{T}_{ik}(\boldsymbol{\mu}, \mathbf{f})$	Task offloading latency from user n_i to UAV u_k
$\mathbf{f}_k \triangleq [f_{1k}, \dots, f_{N_m k}]$	Computing resource allocation decision at u_k	f_{ij}	Computational speed allocated to n_i at u_k
$\mathcal{E}_k^{\text{comp}}(\boldsymbol{\mu}, \mathbf{f})$	Computing energy consumption of the CPU of UAV u_k	$\mathcal{E}_k^{\text{tra}}(\boldsymbol{\mu}, \psi, \mathbf{P})$	Transmission energy consumption of UAV u_k
$\mathcal{E}_k(\boldsymbol{\eta}, \boldsymbol{\mu}, \psi, \mathbf{f}, \mathbf{P})$	Total energy consumption of UAV u_k	z^{\min}/z^{\max}	Minimum/maximum allowable altitude limits of UAV u_k
$\mathcal{G} \triangleq \{\mathcal{V}, \mathcal{E}, \mathcal{W}\}$	Graph model with \mathcal{V} vertices, \mathcal{E} edges, and \mathcal{W} weight of the edges	$\mathcal{V}^c/\mathcal{V}^s/\mathcal{V}^m$	Vertices sets of content/sensing/ MEC users
$w_{ik}(\ell)$	The weight of the edge i, k at the ℓ -th step	\mathcal{V}^u	Vertices sets of the UAVs
Q	Number of iterations in Algorithm 3	I	The amount of the required information by the sensing tenant

Various works in the literature have considered UAV-enabled MEC and network slicing. In [17], a collaborative multi-UAV decision-making system was considered to optimize the task offloading and resource allocation in MEC networks. The objective was to reduce the task computing delay and energy consumption under constraints on allowable task completion time and compliance with resource limitations. A two-stage optimization algorithm was developed to optimize the task offloading decision and resource allocation of the collaborative computing system. In [18], a hierarchical aerial MEC network architecture was considered to improve the quality of user experiences. A bi-level UAV-enabled MEC network was deployed to provide continuous MEC services to ground users with variable demands. An optimization problem was formulated to minimize the utility of all users. The stability of task queue backlogs and energy consumption budgets at users and UAVs were considered. In [19], a multi-domain network slicing scheme for satellite-airborne-terrestrial

edge computing networks was considered. Each slice has configured to include terrestrial-airborne, terrestrial-satellite, or terrestrial-airborne-satellite domain typologies based on the resources availability. The paper optimized the slice configuration selection, routing, and resource allocation. In [20], a UAV network slicing framework was considered in which a system controller can turn on and off the computing elements at the UAVs, with the possibility of offloading jobs to other UAVs. In [15], a hierarchical UAV slicing framework that operates at two different time-scales was studied. The problem of inter-slice resource management was formulated as a mixed integer nonlinear program and a stochastic game with the objective of maximizing the total transmission rate. The aforementioned works did not consider providing multiple services using a shared UAV networks, with each service has its own requirements.

This paper develops a framework to enable a content dissemination tenant, a sensing data gathering tenant, and an MEC tenant to share a set of UAVs to provide services to their users. The content dissemination tenant aims to deliver the required content to each of its subscribers or users. The objective of the sensing data gathering tenant is to gather a sufficient amount of uncorrelated data from his users while the MEC tenant provides computing services. The developed framework enables the software-defined networking (SDN)/ network function virtualization (NFV) controller to satisfy the tenants' requirements with minimum energy consumption. As the network conditions and/or the tenants' requirements change, the developed framework enables the SDN/NFV to decide the number of deployed UAVs and their deployment locations, allocate the transmitted power and the computation resources of the deployed UAVs, select the active sensing devices, and obtain the user-UAV association. The main contributions of this paper can be summarized as follows:

- A network slicing framework is developed to share a multi-UAV network by content dissemination, sensing data gathering, and MEC tenants.
- An energy minimization problem is formulated to guarantee that all the required contents are delivered, sufficient information is gathered, and all the MEC users are served. The UAVs' deployment locations, the UAVs' power allocation, computing resources allocation, and the user-UAV association are optimized. Considering the spatial correlation among the users and the trade-off between the consumed energy and the number of active sensing users, the sensing users' activation is also optimized.

- A solution inherited from graph theory is devised, in which the Lagrange approach derives the transmission power and computing resource allocation expressions.

The remainder of this paper is organized as follows. Section II presents the considered system model and discusses data gathering, communication, and energy consumption models. In Section III, the energy consumption minimization problem is formulated. Section IV introduces the proposed heuristic solution. Section V discusses the simulation results, and Section VI concludes the paper.

Notation: Lower case and upper case boldface letters denote vectors and matrices, respectively. $(\cdot)^H$ and $(\cdot)^T$ represent the Hermitian and the transpose operators, respectively. The main notations used throughout this paper are summarized in Table I.

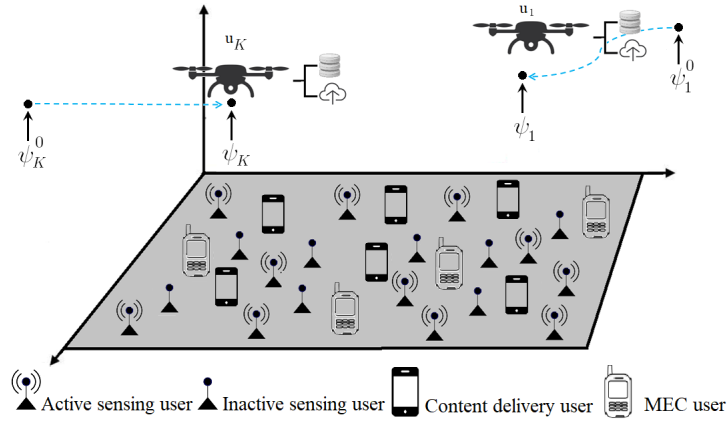


Fig. 1. System model with $K \leq U$ deployed UAVs.

II. System Model

As shown in Fig. 1, a network slicing framework is considered where three tenants (i.e., services) provide content delivery, sensing data gathering, and MEC services to a set of $\mathcal{N} = \{n_i\}_{i=1}^N$ of N users. The UAV-enabled network consists of a set $\mathcal{U} = \{u_k\}_{k=1}^U$ of U UAVs; each UAV operates in full duplex mode with a maximum transmit power P_k , computing speed F_k , and A_k antennas. The tenants share K UAVs, where $K \leq U$ is the number of deployed UAVs. Each tenant serves its own subset of users $\mathcal{N} = \{\mathcal{N}_c, \mathcal{N}_s, \mathcal{N}_m\}$, where $\mathcal{N}_c = \{n_i\}_{i=1}^{N_c}$ represents the content delivery users, $\mathcal{N}_s = \{n_i\}_{i=N_c+1}^{N_c+N_s}$ is the set of sensing users, and $\mathcal{N}_m = \{n_i\}_{i=N_c+N_s+1}^N$ is the MEC users where $N = N_c + N_s + N_m$. The content delivery tenant serves its users by delivering a catalog $\mathcal{C} = \{c_j\}_{j=1}^C$ of C contents

each of size M_j bits. A content delivery user is interested in downloading a content. To represent the users' content demand, let us define $\mathbf{R} = [r_{ij}]_{N_c \times C}$ such that

$$r_{ij} = \begin{cases} 1, & \text{if } n_i \text{ is interested in downloading } c_j, \\ 0, & \text{otherwise.} \end{cases} \quad (1)$$

Furthermore, let us define the UAVs' content storage indicator $\mathbf{S} = [s_{jk}]_{C \times U}$ such that

$$s_{jk} = \begin{cases} 1, & \text{if } c_j \text{ is stored in } u_k, \\ 0, & \text{otherwise.} \end{cases} \quad (2)$$

Additionally, $\sum_{j=1}^C s_{jk} \geq 1, \forall c_j \in \mathcal{C}$ to reflect the fact that each content should be stored in at least one UAV.

The sensing tenant gathers data from its users, where each user can obtain L bits of raw data. Activating all the users is an inefficient approach as their data could be correlated; this approach yields more interference at the UAVs and increases their travelling and hovering time. The spatial correlation, which is a result of the close proximity between the sensing users, is the main cause of data correlation. Consequently, the sensing tenant aims at gathering uncorrelated data (referred to as information in this paper). An empirical study has been performed in [21] to quantify the total gathered information from a set of N_s sensing users using a constructive iterative approach. Since a sensing user generates L (bits) of raw data, the information provided by the first sensing user is $\mathcal{H}_1 = L$ (bits). The information collected by the first and second active sensing users can be obtained as $\mathcal{H}_2 = L + \left[1 - \frac{1}{(\bar{d}_{1,2}/\rho + 1)}\right] L$, where $\bar{d}_{1,2}$ is the Euclidean distance between the locations of the first and second active sensing users and ρ is a parameter that depends on the correlation extent in the sensed data [21]. The information of the first three active sensing users can be obtained as

$$\mathcal{H}_3 = L + \left[1 - \frac{1}{(\bar{\bar{d}}_2/\rho + 1)}\right] L + \left[1 - \frac{1}{(\bar{\bar{d}}_3/\rho + 1)}\right] L, \quad (3)$$

where $\bar{\bar{d}}_2 = \bar{d}_{1,2}$ and $\bar{\bar{d}}_3 = \min\{\bar{d}_{1,3}, \bar{d}_{2,3}\}$. Consequently, the maximum information that can be gathered by N_s sensing users can be expressed as

$$H = L + L \sum_{i=2}^{N_s} \left[1 - \frac{1}{\bar{\bar{d}}_i/\rho + 1}\right], \quad (4)$$

where \bar{d}_i is the minimum distance between the location of the sensing user n_i and all other previously considered users $n_\ell \forall \ell = 1, 2, \dots, i-1$. Let us define the sensing users activation decision $\boldsymbol{\eta} = [\eta_i]_{N_s \times 1}$ such that

$$\eta_i = \begin{cases} 1, & \text{if } n_i \text{ is active,} \\ 0, & \text{otherwise.} \end{cases} \quad (5)$$

For a given sensing users activation decision $\boldsymbol{\eta}$, the gathered information of the active sensing users (users with $\eta_i = 1$) can be obtained as

$$\mathcal{H}(\boldsymbol{\eta}) = L + L \sum_{i=2}^{N_s} \eta_i \left[1 - \frac{1}{d_i(\boldsymbol{\eta})/\rho + 1} \right], \quad (6)$$

where $d_i(\boldsymbol{\eta})$ is the minimum distance between the location of active user n_i and all active users with $\eta_\ell = 1 \forall \ell = 1, 2, \dots, i-1$.

Each MEC user offloads a task $\{\ell_i, \varsigma_i\} \forall n_i \in \mathcal{N}_m$, where ℓ_i is the task size (in bits) and ς_i is the number of CPU cycles required to compute one bit.

A. Communication Model

The communication channel between a user n_i and a UAV u_k is modelled as

$$\mathbf{h}_{ik} = \sqrt{\lambda_0 d_{ik}^{-\beta}} \left[\sqrt{\frac{F}{F+1}} \tilde{\mathbf{h}}_{ik}^{\text{LoS}} + \sqrt{\frac{1}{F+1}} \tilde{\mathbf{h}}_{ik}^{\text{NLoS}} \right], \quad (7)$$

where $d_{ik} = \|\psi_k - \bar{\psi}_i\|$ is the distance between the user n_i and UAV u_k , where $\psi_k = \{x_k, y_k, z_k\}$ are the Cartesian coordinates of the placement location of u_k and $\bar{\psi}_i = \{\bar{x}_i, \bar{y}_i, 0\}$ represent the Cartesian coordinates of user n_i . λ_0 is the path loss at the reference distance of 1 meter, β is the path loss exponent, F denotes the Rician factor, $\tilde{\mathbf{h}}_{ik}^{\text{NLoS}} \in \mathbb{C}^{A_k \times 1}$ represents the non-line-of-sight scattering components modelled by independent random Rayleigh distributed entries, and $\tilde{\mathbf{h}}_{ik}^{\text{LoS}} \in \mathbb{C}^{A_k \times 1}$ is the LoS component. By considering a uniform linear array with the inter-element spacing being one-half the carrier wavelength, the LoS component of the channel from the device n_i to the UAV-mounted server u_k is modelled as

$$\tilde{\mathbf{h}}_{ik}^{\text{LoS}} = [1, e^{-\sqrt{-1}\pi \cos \phi_{ik}}, \dots, e^{-\sqrt{-1}\pi(A_k-1) \cos \phi_{ik}}], \quad (8)$$

where ϕ_{ik} is the angle between user n_i and the UAV u_k , such that $\cos \phi_{ik} = \frac{x_k - \bar{x}_i}{\|\psi_k - \bar{\psi}_i\|}$. Each UAV operates on its orthogonal channel and is deployed to serve a subset of users $\mathcal{N}_k \subseteq \mathcal{N}$,

such that $\bigcup_{k=1}^K \mathcal{N}_k = \mathcal{N}$. Let us define the user-UAV association decision $\boldsymbol{\mu} = [\mu_{ik}]_{N \times U}$ such that

$$\mu_{ik} = \begin{cases} 1, & \text{if } n_i \text{ is served by } u_k, \\ 0, & \text{otherwise.} \end{cases} \quad (9)$$

Let $\mathbf{P} \triangleq [\mathbf{p}_1, \dots, \mathbf{p}_K]$ with $\mathbf{p}_k = [P_{1k}, \dots, P_{Nk}]^T$ as the UAV transmit power allocation decision of UAV u_k , the signal-to-interference-plus-noise ratio (SINR) at user n_i to decode the message sent by u_k can be expressed as

$$\gamma_{ik}(\boldsymbol{\mu}, \boldsymbol{\psi}, \mathbf{P}) = \frac{\mu_{ik} P_{ik} |\mathbf{h}_{ik}^H \mathbf{w}_{ik}|^2}{\sum_{\substack{i'=1 \\ i' \neq i}}^N \mu_{i'k} P_{i'k} |\mathbf{h}_{ik}^H \mathbf{w}_{i'k}|^2 + \sigma_i^2}, \quad (10)$$

where P_{ik} is the allocated power by the UAV u_k to communicate with user n_i and \mathbf{w}_{ik} is the beamforming vector, which can be obtained using the maximum ratio transmission scheme as follows

$$\mathbf{w}_{ik} = \frac{\mathbf{h}_{ik}}{\|\mathbf{h}_{ik}\|}. \quad (11)$$

The corresponding data rate is

$$\mathcal{R}_{ik}(\boldsymbol{\mu}, \boldsymbol{\psi}, \mathbf{P}) = B_k \log_2 (1 + \gamma_{ik}(\boldsymbol{\mu}, \boldsymbol{\psi}, \mathbf{P})), \quad (12)$$

where B_k is the downlink bandwidth of UAV u_k . The SINR of user n_i at UAV u_k can be expressed as

$$\bar{\gamma}_{ik}(\boldsymbol{\eta}, \boldsymbol{\mu}, \boldsymbol{\psi}) = \frac{\eta_i \mu_{ik} \bar{P}_i |\mathbf{h}_{ik}^H \bar{\mathbf{w}}_{ik}|^2}{\sum_{\substack{\iota=1 \\ \iota \neq i}}^N \eta_\iota \mu_{\iota k} \bar{P}_\iota |\mathbf{h}_{ik}^H \bar{\mathbf{w}}_{\iota k}|^2 + \sigma_k^2}, \quad (13)$$

where \bar{P}_i is the transmitted power of user n_i and $\bar{\mathbf{w}}_{ik}$ is the beamforming vector, which can be obtained using the maximum ratio combining scheme. The uplink bandwidth is \bar{B}_k , and thus the data rate from n_i to u_k is expressed as

$$\bar{\mathcal{R}}_{ik}(\boldsymbol{\eta}, \boldsymbol{\mu}, \boldsymbol{\psi}) = \bar{B}_k \log_2 (1 + \bar{\gamma}_{ik}(\boldsymbol{\eta}, \boldsymbol{\mu}, \boldsymbol{\psi})). \quad (14)$$

B. Energy Consumption Model

The UAV consumes its energy to realize the following primary functions: travelling, hovering, and communication. According to [22], the movement power consumption of a UAV can be modelled as

$$P^{(\text{mov})} = P^{(\text{prof})} \left[1 + \frac{3V^2}{\varpi^2} \right] + P^{(\text{ind})} \left[\sqrt{1 + \frac{V^4}{4v_0^4}} - \frac{V^2}{2v_0^2} \right]^{\frac{1}{2}} + \frac{1}{2} \delta_0 \varsigma \zeta \xi V^3, \quad (15)$$

where V is the travelling speed of the UAV, $P^{(\text{prof})}$ and $P^{(\text{ind})}$ are the power of the blade profile and induced power in hovering status, respectively. The rotor blade's tip speed is represented by ϖ , v_0 is the hovering mean rotor-induced velocity, δ_0 and ζ denote the fuselage drag ratio and rotor solidity, respectively. Finally, ς and ξ represent the air density and rotor disc area, respectively. It is worth mentioning that the power consumed by the UAV in hovering $P^{(\text{hov})}$ can be obtained by setting $V = 0$ in (15), which leads to $P^{(\text{hov})} = P^{(\text{prof})} + P^{(\text{ind})}$ [22]. Consequently, the energy consumption of flying UAV u_k from its docking location ψ_k^0 to the placement location ψ_k is modeled as [22], [23]

$$\mathcal{E}_k^{\text{mov}}(\boldsymbol{\psi}) = \frac{P^{(\text{mov})}}{V} \|\psi_k^0 - \psi_k\|. \quad (16)$$

The energy consumption of the UAV u_k while hovering at its placement location can be expressed as

$$\mathcal{E}_k^{\text{hov}}(\boldsymbol{\eta}, \boldsymbol{\mu}, \boldsymbol{\psi}, \mathbf{f}, \mathbf{P}) = P^{(\text{hov})} \max_{\forall n_i \in \mathcal{N}} \left\{ \frac{\mu_{ik} \sum_{j=1}^C r_{ij} M_j}{\mathcal{R}_{ik}(\boldsymbol{\mu}, \boldsymbol{\psi}, \mathbf{P})}, \frac{\eta_i \mu_{ik} L}{\bar{\mathcal{R}}_{ik}(\boldsymbol{\eta}, \boldsymbol{\mu}, \boldsymbol{\psi})}, \mathcal{T}_{ik}(\boldsymbol{\mu}, \mathbf{f}) \right\}, \quad (17)$$

where $\mathcal{T}_{ik}(\boldsymbol{\mu}, \mathbf{f})$ is the offloading latency which can be expressed as

$$\mathcal{T}_{ik}(\boldsymbol{\mu}, \mathbf{f}) = \begin{cases} \mu_{ik} \left(\frac{\ell_i}{\mathcal{R}_{ik}} + \frac{\ell_i \varsigma_i}{f_{ik}} \right), & \forall n_i \in \mathcal{N}_m, \\ 0, & \text{otherwise,} \end{cases} \quad (18)$$

where f_{ij} is the computational speed allocated to n_i at u_k (cycle per second). The computing resource allocation decision at u_k is $\mathbf{f}_k \triangleq [f_{1k}, \dots, f_{N_m k}]$, which satisfies $\sum_{i=1}^{N_m} f_{ik} \leq F_k$, where F_k is the total computing resource of u_k . The computing power consumption can be modeled as $P^{(\text{comp})} = \kappa f^3$, where f is the CPU's computational speed and κ is the effective switched capacitance depending on the CPU chip architecture [24]. Consequently, the computing energy consumption of the CPU of u_k is expressed as

$$\mathcal{E}_k^{\text{comp}}(\boldsymbol{\mu}, \mathbf{f}) = \kappa \sum_{i=1}^{N_m} \ell_i \varsigma_i f_{ik}^2 \mu_{ik}^{\bar{\varsigma}}, \quad (19)$$

where $\tilde{i} = i + N_c + N_s$. The total energy consumed by UAV u_k can be expressed as

$$\mathcal{E}_k(\boldsymbol{\eta}, \boldsymbol{\mu}, \boldsymbol{\psi}, \mathbf{f}, \mathbf{P}) = \mathcal{E}_k^{\text{mov}}(\boldsymbol{\psi}) + \mathcal{E}_k^{\text{hov}}(\boldsymbol{\eta}, \boldsymbol{\mu}, \mathbf{f}, \mathbf{P}) + \mathcal{E}_k^{\text{comp}}(\boldsymbol{\mu}, \mathbf{f}) + \underbrace{\sum_{i=1}^{N_c} \frac{P_{ik} \mu_{ik} \sum_{j=1}^C r_{ij} M_j}{\mathcal{R}_{ik}(\boldsymbol{\mu}, \boldsymbol{\psi}, \mathbf{P})}}_{\mathcal{E}_k^{\text{tra}}(\boldsymbol{\mu}, \boldsymbol{\psi}, \mathbf{P})}, \quad (20)$$

where $\mathcal{E}_k^{\text{tra}}(\boldsymbol{\mu}, \boldsymbol{\psi}, \mathbf{P})$ is the transmission energy consumed by the transmitter circuitry of UAV u_k . The energy consumed by the UAV's receiver circuitry is very small, and it can be neglected.

III. Problem Formulation

Let $I \leq H$ (in bits) be the minimum amount of information required to be aggregated to meet the sensing tenant requirement. The decision-makers need to satisfy the requirements of the tenants (aggregate the required information, deliver all the required contents, and compute the offloaded tasks). The objective is to minimize the energy consumption by deciding the number of deployed UAVs $K \leq U$ and their deployment locations $\boldsymbol{\psi}$, selecting the active sensing devices $\boldsymbol{\eta}$, allocating the transmitted power \mathbf{P} and the computation resources \mathbf{f} , and determining the user-UAV association $\boldsymbol{\mu}$. The optimization problem is formulated as follows:

$$\text{P1 } \min_{\substack{\boldsymbol{\eta}, \boldsymbol{\mu}, \boldsymbol{\psi} \\ \mathbf{P}, \mathbf{f}, K}} \sum_{k=1}^K \mathcal{E}_k(\boldsymbol{\eta}, \boldsymbol{\mu}, \boldsymbol{\psi}, \mathbf{f}, \mathbf{P}), \quad (21a)$$

$$\text{s.t. } \sum_{k=1}^U \mu_{ik} \geq 1, \quad 1 \leq i \leq N_c, \quad (21b)$$

$$\sum_{k=1}^U \sum_{j=1}^C \mu_{ik} s_{jk} r_{ij} = \sum_{j=1}^C r_{ij}, \quad 1 \leq i \leq N_c, \quad (21c)$$

$$\sum_{k=1}^U \mu_{ik} = \eta_i, \quad N_c + 1 \leq i \leq N_c + N_s, \quad (21d)$$

$$\mathcal{H}(\boldsymbol{\eta}) \geq I, \quad (21e)$$

$$\sum_{i=1}^{N_c} \mu_{ik} P_{ik} \leq P_k, \quad \forall u_k \in \mathcal{U}, \quad (21f)$$

$$\sum_{k=1}^U \mu_{ik} = 1, \quad N_c + N_s \leq i \leq N, \quad (21g)$$

$$\sum_{i=1}^{N_m} \mu_{ik}^{\bar{z}} f_{ik} \leq F_k, \quad \forall u_k \in \mathcal{U}, \quad (21h)$$

$$z^{\min} \leq z_k \leq z^{\max}, \quad 1 \leq k \leq K, \quad (21i)$$

$$K \leq U, \mu_{ik} \text{ and } \eta_i \in \{0, 1\}, \quad \forall n_i \in \mathcal{N}, u_k \in \mathcal{U}. \quad (21j)$$

Constraints (21b) and (21c) guarantee that each content delivery user is served by one or more UAVs that store the requested contents, respectively. Constraint (21d) guarantees that each active sensing user is served by one UAV. Constraint (21e) guarantees that sufficient information is gathered. Constraint (21f) represents the maximum transit power limit of each UAV. Constraints (21g) and (21h) guarantee that each MEC user is associated with a UAV and each UAV allocates the available computation resources, respectively. Constraint (21i) guarantees that each deployed UAV hovers within the allowable altitude limits.

IV. Proposed Solution Approach

In this section, a heuristic solution is developed to solve the formulated optimization problem using techniques inherited from the graph theory and the Lagrange approach. The proposed algorithm is a problem-specific approach that is designed based on the structure of the optimization problem, and it provides near-optimum energy consumption

minimization in the considered system model. The proposed algorithm optimizes multiple decision variables including the number of deployed UAVs $K \leq U$, their deployment locations $\boldsymbol{\psi}$ and the active sensing devices $\boldsymbol{\eta}$; allocates the transmitted power P and the computation resources f ; and determines the user-UAV association $\boldsymbol{\mu}$. The computation complexity of the algorithm is discussed in Section IV.D.

A. Optimizing the Transmission Power Allocation

For a given $\boldsymbol{\eta}, \boldsymbol{\mu}, \boldsymbol{\psi}, f$, and K , the transmit power allocation of UAV u_k can be obtain by solving the following optimization problem

$$\text{P1-P} \min_{P_k} \max_{\forall n_i \in \mathcal{N}_c} \left\{ P^{(\text{hov})} \mu_{ik} \frac{\sum_{j=1}^C r_{ij} M_j}{\mathcal{R}_{ik}}, E_2 \right\} + \sum_{i=1}^{N_c} P_{ik} \mu_{ik} \frac{\sum_{j=1}^C r_{ij} M_j}{\mathcal{R}_{ik}}, \quad (22a)$$

$$\text{s.t.} \quad \sum_{i=1}^{N_c} \mu_{ik} P_{ik} \leq P_k, \quad (22b)$$

$$P_{ik} \geq 0 \quad \forall n_i \in \mathcal{N}_c, \quad (22c)$$

where E_2 is a constant and can be obtained as follows

$$E_2 = P^{(\text{hov})} \max_{\forall n_i \in \mathcal{N}} \left\{ \frac{\eta_i \mu_{ik} L}{\mathcal{R}_{ik}(\boldsymbol{\eta}, \boldsymbol{\mu}, \boldsymbol{\psi})}, \mathcal{T}_{ik}(\boldsymbol{\mu}, f) \right\}. \quad (23)$$

By introducing the auxiliary variables $\boldsymbol{\tau} \triangleq \{\tau_1, \dots, \tau_{N_c}\}$ and ϱ , the optimization problem P1-P can be rewritten as

$$\text{P2-P} \min_{\mathbf{P}_k, \boldsymbol{\tau}, \varrho} \quad \varrho + \frac{1}{P^{(\text{hov})}} \sum_{i=1}^{N_c} P_{ik} \tau_i, \quad (24\text{a})$$

$$\text{s.t.} \quad P^{(\text{hov})} \mu_{ik} \frac{\sum_{j=1}^C r_{ij} M_j}{\mathcal{R}_{ik}} = \tau_i, \forall n_i \in \mathcal{N}_c, \quad (24\text{b})$$

$$\tau_i \leq \varrho, \forall n_i \in \mathcal{N}_c, \quad (24\text{c})$$

$$E_2 \leq \varrho, \quad (24\text{d})$$

$$\sum_{i=1}^{N_c} \mu_{ik} P_{ik} \leq P_k, \quad (24\text{e})$$

$$P_{ik} \geq 0 \quad \forall n_i \in \mathcal{N}_c. \quad (24\text{f})$$

The corresponding Lagrangian function can be written as

$$\begin{aligned} \mathcal{L}(\mathbf{P}_k, \boldsymbol{\tau}, \varrho, \boldsymbol{\nu}) &= \varrho + \frac{1}{P^{(\text{hov})}} \sum_{i=1}^{N_c} P_{ik} \tau_i + \sum_{i=1}^{N_c} \bar{\nu}_i (\tau_i - \varrho) \\ &+ \sum_{i=1}^{N_c} \nu_i \left(P^{(\text{hov})} \mu_{ik} \sum_{j=1}^C r_{ij} M_j - \tau_i \mathcal{R}_{ik} \right) + \bar{\bar{\nu}} (E_2 - \varrho), \end{aligned} \quad (25)$$

where $\boldsymbol{\nu} \triangleq \{\nu_i, \bar{\nu}_i, \bar{\bar{\nu}}\}$ are the Lagrangian multipliers. The Lagrange dual function can be written as [25, Sec. 5.1.2]

$$\mathcal{D}(\boldsymbol{\nu}) = \min_{\mathbf{P}_k, \boldsymbol{\tau}, \varrho} \mathcal{L}(\mathbf{P}_k, \boldsymbol{\tau}, \varrho, \boldsymbol{\nu}). \quad (26)$$

Further, the dual problem can be expressed as

$$\max_{\boldsymbol{\nu}} \quad \mathcal{D}(\boldsymbol{\nu}) \quad (27\text{a})$$

$$\text{s.t.} \quad \bar{\nu}_i, \bar{\bar{\nu}} \geq 0. \quad (27\text{b})$$

The optimum solution should satisfy the following conditions

$$\begin{aligned}
\frac{\partial \mathcal{L}(P_k, \boldsymbol{\tau}, \varrho, \boldsymbol{\nu})}{\partial P_{ik}} &= \frac{\tau_i^*}{P^{(\text{hov})}} - \nu_i^* \tau_i^* \mathcal{R}'_{ik} = 0, \\
\frac{\partial \mathcal{L}(P_k, \boldsymbol{\tau}, \varrho, \boldsymbol{\nu})}{\partial \tau_i} &= \frac{P_{ik}^*}{P^{(\text{hov})}} - \nu_i^* \mathcal{R}_{ik} + \bar{\nu}_i^* = 0, \\
\frac{\partial \mathcal{L}(P_k, \tau_i, \varrho, \boldsymbol{\nu})}{\partial \nu_i} &= P^{(\text{hov})} \sum_{j=1}^C r_{ij} M_j - \tau_i^* \mathcal{R}_{ik} = 0, \\
P_{ik}^* &\geq 0,
\end{aligned} \tag{28}$$

where $\mathcal{R}'_{ik} \triangleq \frac{\partial \mathcal{R}_{ik}}{\partial P_{ik}} = \frac{B|\mathbf{h}_{ik}^H \mathbf{w}_{ik}|^2}{P_{ik}^* |\mathbf{h}_{ik}^H \mathbf{w}_{ik}|^2 + \omega_i}$, with $\omega_i = \sum_{\substack{i'=1 \\ i' \neq i}}^N P_{i'k}^* |\mathbf{h}_{ik}^H \mathbf{w}_{i'k}|^2 + \sigma_i^2$. By setting $\varrho = \tau_i$ and $\bar{\nu}_i^* = 0$, the power allocation can be obtained using (28) as follows

$$P_{ik}^* = \begin{cases} \frac{P^{(\text{hov})} \omega_i \sum_{j=1}^C r_{ij} M_j}{\varrho^* B |\mathbf{h}_{ik}^H \mathbf{w}_{ik}|^2 - P^{(\text{hov})} \sum_{j=1}^C r_{ij} M_j}, & \text{if } \mu_{ik} = 1, \\ 0, & \text{otherwise.} \end{cases} \tag{29}$$

Finally, it can be noticed that P_{ik} is monotonically decreasing with respect to ϱ and the feasibility range of ϱ is $\varrho^* \in [\varrho_{\min}, \varrho_{\max}]$. The lower limit can be obtained as

$$\varrho_{\min} = \max\{E_2, \frac{P^{(\text{hov})}}{B |\mathbf{h}_{ik}^H \mathbf{w}_{ik}|^2} \sum_{j=1}^C r_{ij} M_j \forall n_i \in \mathcal{N}_c\}. \tag{30}$$

The upper limit can be obtained as follows. Let us define ϱ_P as the value that satisfies (24b) and (24c), which corresponds to equally allocate the transmission power and can be expressed as follows

$$\varrho_P = \max_{\forall n_i \in \mathcal{N}_c} \left\{ P^{(\text{hov})} \frac{\sum_{j=1}^C r_{ij} M_j}{R_{ik}} \right\}, \tag{31}$$

where R_{ik} is the data rate of equally allocate the transmission power (i.e., $P_{ik} = P_k/N_c$). The upper limit can be obtained as $\varrho_{\max} = \max\{\varrho_P, E_2\}$. Algorithm 1 illustrates the procedure of solving Problem P1-P.

Algorithm 1 Transmission power allocation.

```

1: Input:  $\boldsymbol{\eta}, \boldsymbol{\mu}, \boldsymbol{\psi}, f_k, P_k$ , and  $\epsilon$ ;
2: Initialize:  $\varrho_{\min} = E_2$ ;  $P_{ik} = P_k/N_c$ ; Obtain  $\varrho_P$  using (31);  $\varrho_{\max} = \max\{\varrho_P, E_2\}$ ; Set  $\varrho^* \leftarrow \varrho_{\max}$ ;
3: Obtain  $P_{ik}^*, \forall n_i \in \mathcal{N}_c$  using (29);
4: While  $|\varrho_{\max} - \varrho_{\min}| > \epsilon$  do:
5:    $\varrho = \frac{\varrho_{\max} + \varrho_{\min}}{2}$ ;
6:   Obtain  $P_{ik}, \forall n_i \in \mathcal{N}_c$  using (29);
7:   If  $\sum_{i=1}^{N_c} P_{ik} \leq P_k$  and  $P_{ik} \geq 0 \forall n_i \in \mathcal{N}_c$  do:
8:      $\varrho_{\max} \leftarrow \varrho$ ;
9:      $P_{ik}^* \leftarrow P_{ik}$ ;
10:  Else do
11:     $\varrho_{\min} \leftarrow \varrho$ ;
12:  End If
13: Return  $P_{ik}^*, \forall n_i \in \mathcal{N}_c$ .

```

B. Optimizing the Computing Resources

For a given $\boldsymbol{\eta}, \boldsymbol{\mu}, \boldsymbol{\psi}, P$, and K , the edge computing resource of UAV u_k can be obtain by solving the following optimization problem

$$\text{P1-f } \min_{f_k} \max_{\forall n_i \in \mathcal{N}} \left\{ P^{(\text{hov})} \mu_{ik} \left(\frac{\ell_{\tilde{i}}}{\mathcal{R}_{\tilde{i}k}} + \frac{\ell_{\tilde{i}} \zeta_{\tilde{i}}}{f_{\tilde{i}k}} \right), E_1 \right\} + \kappa \sum_{i=1}^{N_m} \ell_{\tilde{i}} \zeta_{\tilde{i}} f_{\tilde{i}k}^2 \mu_{ik}, \quad (32a)$$

$$\text{s.t. } \sum_{i=1}^{N_m} \mu_{ik} f_{\tilde{i}k} \leq F_k, \quad (32b)$$

$$f_{\tilde{i}k} \geq 0 \quad \forall n_i \in \mathcal{N}_m, \quad (32c)$$

where E_1 is a constant and can be obtained as follows

$$E_1 = P^{(\text{hov})} \max_{\forall n_i \in \mathcal{N}} \left\{ \frac{\mu_{ik} \sum_{j=1}^C r_{ij} M_j}{\mathcal{R}_{ik}(\boldsymbol{\mu}, \boldsymbol{\psi}, P)}, \frac{\eta_i \mu_{ik} L}{\mathcal{R}_{ik}(\boldsymbol{\eta}, \boldsymbol{\mu}, \boldsymbol{\psi})} \right\}. \quad (33)$$

By introducing the auxiliary variable λ , the optimization problem P1-f can be rewritten as follows

$$\text{P2-f } \min_{\mathbf{f}_k, \lambda} \quad \lambda + \kappa \sum_{i=1}^{N_m} \ell_{\bar{z}\zeta_i} f_{ik}^2 \mu_{\bar{z}ik}, \quad (34a)$$

$$\text{s.t. } P^{(\text{hov})} \mu_{\bar{z}ik} \left(\frac{\ell_{\bar{z}i}}{\mathcal{R}_{\bar{z}ik}} + \frac{\ell_{\bar{z}\zeta_i}}{f_{ik}} \right) \leq \lambda, \forall n_i \in \mathcal{N}_m \quad (34b)$$

$$E_1 \leq \lambda, \quad (34c)$$

$$\sum_{i=1}^{N_m} \mu_{\bar{z}ik} f_{ik} \leq F_k, \quad (34d)$$

$$f_{\bar{z}ik} \geq 0 \quad \forall n_i \in \mathcal{N}_m. \quad (34e)$$

The corresponding Lagrangian function can be written as

$$\mathcal{L}(\mathbf{f}_k, \lambda, \boldsymbol{\chi}) = \lambda + \kappa \sum_{i=1}^{N_m} \ell_{\bar{z}\zeta_i} f_{ik}^2 \mu_{\bar{z}ik} + \chi_1 (E_1 - \lambda) + \sum_{i=1}^{N_m} \bar{\chi}_i \left(P^{(\text{hov})} \mu_{\bar{z}ik} \left(\frac{\ell_{\bar{z}i}}{\mathcal{R}_{\bar{z}ik}} + \frac{\ell_{\bar{z}\zeta_i}}{f_{ik}} \right) - \lambda \right), \quad (35)$$

where $\boldsymbol{\chi} \triangleq \{\chi_1, \bar{\chi}_1, \dots, \bar{\chi}_{N_m}\}$ represents the Lagrangian multipliers. The Lagrange dual function can be expressed as [25, Sec. 5.1.2]

$$\mathcal{D}(\boldsymbol{\chi}) = \min_{\mathbf{f}_k, \lambda} \mathcal{L}(\mathbf{f}_k, \lambda, \boldsymbol{\chi}). \quad (36)$$

The dual problem can be formulated as

$$\max_{\boldsymbol{\chi}} \quad \mathcal{D}(\boldsymbol{\chi}) \quad (37a)$$

$$\text{s.t. } \chi_1, \bar{\chi}_1, \dots, \bar{\chi}_{N_m} \geq 0. \quad (37b)$$

Given that $\mu_{\bar{z}ik}$ is a binary variable and there is no need to allocate computing resources at u_k for the users that are not associated with u_k , it can be deduced that $f_{ik}^* = 0$ for all users with $\mu_{\bar{z}ik} = 0$. For a fixed Lagrangian multipliers and by applying the Karush-Kuhn-Tucker (KKT) conditions and forcing (34b) into equality, a solution for P2-f should satisfy the following conditions

$$\begin{aligned}
\frac{\partial \mathcal{L}(f_k, \lambda, \chi)}{\partial f_{ik}^*} &= 2\kappa \ell_i^* \zeta_i^* f_{ik}^* - \bar{\chi}_i^* P^{(\text{hov})} \frac{\ell_i^* \zeta_i^*}{f_{ik}^{*2}} = 0, \\
\frac{\partial \mathcal{L}(f_k, \lambda, \chi)}{\partial \bar{\chi}_i} &= P^{(\text{hov})} \left(\frac{\ell_i^*}{\bar{\mathcal{R}}_{ik}^*} + \frac{\ell_i^* \zeta_i^*}{f_{ik}^*} \right) - \lambda^* = 0, \\
f_{ik}^* &\geq 0.
\end{aligned} \tag{38}$$

After simple manipulations and keeping in mind that f_{ik}^* is a positive value, a solution for P2-f can be obtained as

$$f_{ik}^* = \begin{cases} \frac{\ell_i^* \zeta_i^* P^{(\text{hov})}}{\lambda^* - P^{(\text{hov})} \frac{\ell_i^*}{\bar{\mathcal{R}}_{ik}^*}}, & \text{if } \mu_{ik}^* = 1, \\ 0, & \text{otherwise.} \end{cases} \tag{39}$$

Finally, it can be noticed that f_{ik}^* is monotonically decreasing with respect to λ and the feasibility range of λ is $\lambda^* \in [\lambda_{\min}, \lambda_{\max}]$. The lower limit can be obtained as $\lambda_{\min} = \max\{E_1, P^{(\text{hov})} \frac{\ell_i^*}{\bar{\mathcal{R}}_{ik}^*} \forall n_i \in \mathcal{N}_m\}$. The upper limit can be obtained as follows. Let us define λ_F as the value that satisfies (34b), which corresponds to equally allocate the available computing resources and can be expressed as follows

$$\lambda_F = \max_{\forall n_i \in \mathcal{N}_m} \left\{ P^{(\text{hov})} \left(\frac{\ell_i^*}{\bar{\mathcal{R}}_{ik}^*} + \frac{\ell_i^* \zeta_i^*}{F_k/N_m} \right) \right\}. \tag{40}$$

The upper limit can be obtained as $\lambda_{\max} = \max\{\lambda_F, E_1\}$. Algorithm 2 illustrates the procedure of solving Problem P1-f.

C. Graph-based Solution

To find the optimized number of deployed UAVs, the sensing users activation, and the user-UAV association, a representation of all feasible solutions should be first designed. A quadripartite graph model is proposed as $\mathcal{G} \triangleq \{\mathcal{V}, \mathcal{E}, \mathcal{W}\}$, where \mathcal{V} represents the vertices, \mathcal{E} represents the edges, and \mathcal{W} is the weight of the edges.

Vertex Set: The vertices set consists of four subsets $\mathcal{V} = \{\mathcal{V}^c, \mathcal{V}^s, \mathcal{V}^m, \mathcal{V}^u\}$. The subset $\mathcal{V}^c \triangleq \{v_i^c\}$ represents the content delivery users such that $|\mathcal{V}^c| = N_c$, $\mathcal{V}^s \triangleq \{v_i^s\}$ represents the sensing users such that $|\mathcal{V}^s| = N_s$, and $\mathcal{V}^m \triangleq \{v_i^m\}$ represents the MEC users such that $|\mathcal{V}^m| = N_m$. The subset $\mathcal{V}^u \triangleq \{v_k^u\}$ represents the UAVs such that $|\mathcal{V}^u| = U$.

Association Edges: Each vertex in the subsets \mathcal{V}^s and \mathcal{V}^m is connected with all the vertices

Algorithm 2 Optimizing the computing resources.

```

1: Input:  $\boldsymbol{\eta}, \boldsymbol{\mu}, \boldsymbol{\psi}, P, F_k$ , and  $\epsilon$ ;
2: Initialize:  $\lambda_{\min} = E_1$ ; Obtain  $\lambda_F$  using (40);  $\lambda_{\max} = \max\{\lambda_F, E_1\}$ ; Set  $\lambda^* \leftarrow \lambda_{\max}$ ;
3: Obtain  $f_{ik}^*$ ,  $\forall n_i \in \mathcal{N}_m$  using (39);
4: While  $|\lambda_{\max} - \lambda_{\min}| > \epsilon$  do:
5:    $\lambda = \frac{\lambda_{\max} + \lambda_{\min}}{2}$ ;
6:   Obtain  $f_{ik}$ ,  $\forall n_i \in \mathcal{N}_m$  using (39);
7:   If  $\sum_{i=1}^{N_m} f_{ik} \leq F_k$  and  $f_{ik} \geq 0 \forall n_i \in \mathcal{N}_m$  do:
8:      $\lambda_{\max} \leftarrow \lambda$ ;
9:      $f_{ik}^* \leftarrow f_{ik}$ ;
10:  Else do
11:     $\lambda_{\min} \leftarrow \lambda$ ;
12:  End If
13: Return  $f_{ik}^*$ ,  $\forall n_i \in \mathcal{N}_m$ .

```

of \mathcal{V}^u as a sensing user or MEC user can be served by any UAV. An edge connects a vertex $v_i^c \in \mathcal{V}^c$ and $v_k^u \in \mathcal{V}^u$ if $r_{ij}s_{jk} = 1$, as the content delivery user can be served only by the UAVs that store its required content. It is worth noting that the total number of vertices in the graph \mathcal{G} is $N + U$, and keeping in mind that \mathcal{G} is quadripartite and no edge is needed within the users' vertices, the number of edges is upper-bounded by NU . This makes the graph size manageable for a reasonably large number of users and UAVs. Figure 2 illustrates an example of the graph model with three UAVs, five sensing users, five content delivery users, and four MEC users. The UAVs' stored contents and the users' demands are as follows

$$\mathbf{R} = \begin{bmatrix} n_1 & n_2 & n_3 & n_4 & n_5 \\ 0 & 0 & 1 & 0 & 0 \\ 0 & 0 & 0 & 0 & 1 \\ 1 & 0 & 0 & 0 & 0 \\ 0 & 1 & 0 & 1 & 0 \end{bmatrix} \begin{matrix} c_1 \\ c_2 \\ c_3 \\ c_4 \end{matrix}; \mathbf{S} = \begin{bmatrix} u_1 & u_2 & u_3 \\ 1 & 1 & 1 \\ 0 & 1 & 0 \\ 1 & 1 & 0 \\ 1 & 0 & 1 \end{bmatrix} \begin{matrix} c_1 \\ c_2 \\ c_3 \\ c_4 \end{matrix}. \quad (41)$$

Edges' Weight: The weight of each edge should reflect the energy consumption of associating the corresponding user and UAV. The weights of the graph $\mathcal{W} = [w_{ik}]_{N \times U}$ are

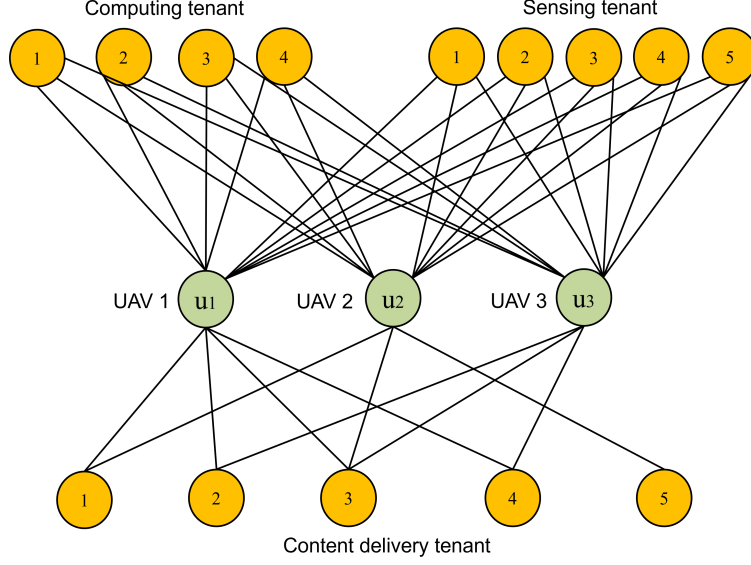


Fig. 2. User-UAV association graph of 3 UAVs, 5 sensing, 4 computing, and 5 content delivery users with the storage and demand in (41).

updated as the users are associated, such that the weight of each edge $w_{ik}(\hat{l})$ at the \hat{l} -th step is assigned as follows

$$w_{ik}(\hat{l}) = \begin{cases} \frac{\Delta(\hat{l})}{\frac{P^{(\text{mov})}d_{ik}(\hat{l})}{V} + \frac{P^{(\text{hov})}L}{\mathcal{R}_{ik}(\hat{l})}}, & \text{if } n_i \in \mathcal{N}_s, \\ \frac{1}{\frac{P^{(\text{mov})}d_{ik}(\hat{l})}{V} + P^{(\text{hov})}\left(\frac{\ell_i}{\mathcal{R}_{ik}^{z_i}(\hat{l})} + \frac{\ell_i s_i}{f_{ik}^{z_i}}\right)}, & \text{if } n_i \in \mathcal{N}_m, \\ \frac{\sum_{j=1}^C r_{ij} s_{jk}}{\frac{P^{(\text{mov})}d_{ik}(\hat{l})}{V} + \frac{(P^{(\text{hov})} + P_{ik}) \sum_{j=1}^C r_{ij} s_{jk} M_j}{\mathcal{R}_{ik}(\hat{l})}}, & \text{if } n_i \in \mathcal{N}_c, \end{cases} \quad (42)$$

where $\Delta(\hat{l}) = 1$ if $\mathcal{H}(\hat{l}) < I$, with $\mathcal{H}(\hat{l})$ as the information gathered by the already associated sensing devices at the \hat{l} -th step; otherwise $\Delta(\hat{l}) = 0$. It is worth noting that the denominators in the first, second, and third lines of (42) represent the energy consumption of associating the UAV u_k with the sensing user, MEC user, and content delivery user n_i , respectively. Consequently, an edge with the highest weight represents the lowest energy consumption of a user-UAV association.

The optimum altitude of the deployed UAV z_k depends on the required effective coverage area, with a circle whose center is (x_k, y_k) and whose radius is the distance between the center and the farthest associated user. Let $\vartheta_{ik} = \sqrt{(\bar{x}_i - x_k)^2 + (\bar{y}_i - y_k)^2}$ be the distance between user n_i and the x - y location of u_k , the optimum altitude can be expressed as

$z_k = \hat{v}_{ik} \tan(\theta_{\text{opt}})$, where $\hat{v}_{ik} = \max_{1 \leq i \leq N} \{\mu_{ik} v_{ik}\}$ and $\theta_{\text{opt}} = 75.52^\circ, 54.62^\circ, 42.44^\circ$, and 20.34° for the high-rise urban, dense urban, urban, and suburban environments, respectively [26]. Keeping in mind the attitude limits in (21h), the altitude of UAV u_k is obtained as follows

$$z_k = \begin{cases} z^{\max}, & \text{if } \hat{v}_{ik} \tan(\theta_{\text{opt}}) \geq z^{\max}, \\ z^{\min}, & \text{if } \hat{v}_{ik} \tan(\theta_{\text{opt}}) \leq z^{\min}, \\ \hat{v}_{ik} \tan(\theta_{\text{opt}}), & \text{otherwise.} \end{cases} \quad (43)$$

Algorithm 3 illustrates the proposed solution approach to solve P1. The algorithm starts with constructing the user-UAV association graph. It is worth noting that according to (42), the initial weights equal zero for the edges between the content delivery users and the UAVs that do not store the corresponding required contents (i.e., $\sum_{j=1}^C r_{ij} s_{jk} = 0$ for each of those edges). The algorithm iterates Q iterations. At each iteration, the algorithm calculates the weights using (42) based on the location of the UAVs and the equally allocated computing resource and transmit power of the UAVs (lines 6-7). The edge with the maximum weight $w_{i\hat{k}}(\hat{i})$ is selected (line 11), user n_i is associated with UAV $u_{\hat{k}}$, and the deployment location of $u_{\hat{k}}$ is updated to be closer to all associated users (lines 11-13). If the associated user is a sensing user, it is set as an active user and the amount of the gathered data is updated (lines 15-17). The corresponding weights of the selected users are set to zero and all the remaining nonzero weights are updated based on the new location of the UAV (lines 18-19). The algorithm continues while there exists an edge with non-zero weight. Once all the users are associated, the transmit power and computing resources of each deployed UAV are obtained using Algorithm 1 and Algorithm 2, respectively (lines 22-23). The algorithm examines the value of the objective function at each iteration and returns the best solution (lines 24-29). It is worth mentioning that once the solution is obtained, the SDN/NFV controller informs each of the deployed UAVs of their deployment location, the user-UAV association, and the transmit power and computation resource allocation decisions.

D. Solution Computational Complexity Analysis

Constructing the user-UAV association graph requires $\mathcal{O}(NU)$ operations, while keeping in mind that $C \leq N$, calculating the corresponding weights using (42) requires $\mathcal{O}(N^2U)$ operations. Obtaining the transmission power allocation using Algorithm 1 requires $\mathcal{O}(\log(\frac{\varrho_{\max} - \varrho_{\min}}{\epsilon})N_c)$

Algorithm 3 A heuristic algorithm for energy-efficient UAV-enabled network slicing.

- 1: Input: $\mathbf{R}, \mathbf{S}, I, \bar{\psi}_i, \forall n_i \in \mathcal{N}, \mathcal{N}, \psi_k(0), P_k, F_k, \forall u_k \in \mathcal{U}$;
- 2: Construct the user-UAV association graph;
- 3: Set $O_{\min} \leftarrow \infty$;
- 4: For $q = 1$ to Q do
- 5: Set $\boldsymbol{\mu} \leftarrow [0]_{N \times U}$ and $\boldsymbol{\eta} \leftarrow [0]_{N_s \times 1}$; $\hat{l} = 0$; $\mathcal{H}(0) = 0$;
- 6: Calculate $d_{ik}(0) = \sqrt{(x_k - \bar{x}_i)^2 + (y_k - \bar{y}_i)^2}$;
- 7: Set $f_{ik} = F_k/N_m$; $P_{ik} = P_k / \sum_{i=1}^{N_c} \sum_{j=1}^C s_{jk} r_{ij}$;
- 8: Obtain $w_{ik}(0) \forall n_i \in \mathcal{N}, \forall u_k \in \mathcal{U}$, using (42);
- 9: While $\exists w_{ik}(\hat{l}) > 0 \forall i = 1, \dots, N, k = 1, \dots, U$ do
- 10: $\hat{l} = \hat{l} + 1$; $d_{ik}(\hat{l}) \leftarrow d_{ik}(\hat{l} - 1)$; $w_{ik}(\hat{l}) \leftarrow w_{ik}(\hat{l} - 1), \forall n_i \in \mathcal{N}, \forall u_k \in \mathcal{U}$;
- 11: Select \hat{i} and \hat{k} such that

$$(\hat{i}, \hat{k}) = \arg \max_{\substack{1 \leq i \leq N \\ 1 \leq k \leq U}} \{w_{ik}(\hat{l})\}.$$

- 12: Set $\mu_{i\hat{k}} = 1$; $x_{\hat{k}}(\hat{l}) = \frac{\sum_{i=1}^N \mu_{i\hat{k}} \bar{x}_i}{\sum_{i=1}^N \mu_{i\hat{k}}}$, $y_{\hat{k}}(\hat{l}) = \frac{\sum_{i=1}^N \mu_{i\hat{k}} \bar{y}_i}{\sum_{i=1}^N \mu_{i\hat{k}}}$;
- 13: $d_{i\hat{k}}(\hat{l}) = \sqrt{(x_{\hat{k}}(\hat{l}) - \bar{x}_i)^2 + (y_{\hat{k}}(\hat{l}) - \bar{y}_i)^2} \forall n_i \in \mathcal{N}$;
- 14: Obtain $z_{\hat{k}}$ using (43);
- 15: If $n_{\hat{i}} \in \mathcal{N}_s$ do
- 16: Set $\eta_{\hat{i}} = 1$; Calculate $\mathcal{H}(\hat{l})$ and $\Delta(\hat{l})$;
- 17: End If
- 18: Set $w_{i\hat{k}}(\hat{l}) = 0 \forall k = 1, \dots, U$;
- 19: Update $w_{ik}(\hat{l})$ if $w_{i\hat{k}}(\hat{l}) \neq 0, \forall n_i \in \mathcal{N}, u_k \in \mathcal{U}$ using (42);
- 20: End While
- 21: Set $K = |\mathcal{K}|$, where \mathcal{K} is a set of deployed UAVs, $u_k \in \mathcal{K}$ if $\exists \mu_{ik} = 1, \forall n_i \in \mathcal{N}$;
- 22: Obtain $P_k \forall u_k \in \mathcal{K}$ using Algorithm 1;
- 23: Obtain $f_k \forall u_k \in \mathcal{K}$ using Algorithm 2;
- 24: Calculate the objective $O = \sum_{k=1}^K \mathcal{E}_k(\boldsymbol{\eta}, \boldsymbol{\mu}, \boldsymbol{\psi}, \mathbf{f}, \mathbf{P})$;
- 25: If $O < O_{\min}$ do
- 26: $O_{\min} = O$; $K^* = K$;
- 27: $\boldsymbol{\mu}^* \leftarrow \boldsymbol{\mu}$; $\boldsymbol{\eta}^* \leftarrow \boldsymbol{\eta}$; $P_k^* \leftarrow P_k$; $f_k^* \leftarrow f_k$; and $\psi_k^* \leftarrow \psi_k$;
- 28: End If
- 29: End For
- 30: Return $K^*, \boldsymbol{\mu}^*, \boldsymbol{\eta}^*, P_k^*, f_k^*$, and ψ_k^* .

operations. Further, optimizing the computing resources using Algorithm 2 requires $\mathcal{O}(\log(\frac{\lambda_{\max}-\lambda_{\min}}{\epsilon})N_m)$ operations. Keeping in mind that $U \leq N$, the computational complexity of solving P1 using Algorithm 3 can be expressed as $\mathcal{O}(Q[N^3 + \log(\frac{\varrho_{\max}-\varrho_{\min}}{\epsilon})N_c + \log(\frac{\lambda_{\max}-\lambda_{\min}}{\epsilon})N_m])$. It is worth noting that the computational complexity of Algorithm 3 is remarkably less than that of obtaining the solution of P1 using exhaustive search (which is described in Section V), which can be expressed as $\mathcal{O}(U^N 2^{N_s} [\log(\frac{\varrho_{\max}-\varrho_{\min}}{\epsilon})N_c + \log(\frac{\lambda_{\max}-\lambda_{\min}}{\epsilon})N_m])$.

V. Simulation Results

This section introduces simulation results to evaluate the considered network slicing framework and the developed graph-based solution. In obtaining these results, it is assumed that the users are randomly placed within a square area of 1.2×1.2 km². One-third of the users are content delivery users, one-third are sensing tenant users, and one-third are MEC users. The content storage capacity of a UAV is set as 75% of the required contents and the content storage indicator matrix \mathbf{S} is obtained as a randomly-generated binary matrix, such that 75% of the elements in each column are ones with the condition that the sum of each row is greater than or equal 1, to ensure that each content is stored at least in one UAV. The content demand matrix \mathbf{R} is obtained as a randomly-generated binary matrix with the condition that the sum of each row equals 1, to ensure that each user requests one content. Each curve in the figures is obtained as the average of 1000 Monte Carlo simulations. Unless otherwise mentioned, Table II summarizes the numerical values of the considered system parameters.

TABLE II
Simulation Parameters.

Parameter	Value	Parameter	Value	Parameter	Value
N	27	U	5	V	12 m/s [22]
P_k	1 W [10]	B_k	1 MHz [10]	F_k	4 GHz
M_j	500 Mbits	ρ	10^2	L	1 Mbits
I	$0.75H$ [3]	F	10 [10]	β	2.2 [10]
λ_0	-30 dB [10]	v_0	4.03 [22]	δ_0	0.6 [22]
ς	1.225 kg/m ³ [22]	ζ	0.05 [22]	ξ	0.503 m ² [22]
ℓ_i	1 Mbits	ς_i	700×10^8 cycle/bit	ϵ	0.01

Figure 3 illustrates the total energy consumption versus the size of the contents M_j . Three solution approaches are illustrated: (I) Random solution: in which all the available

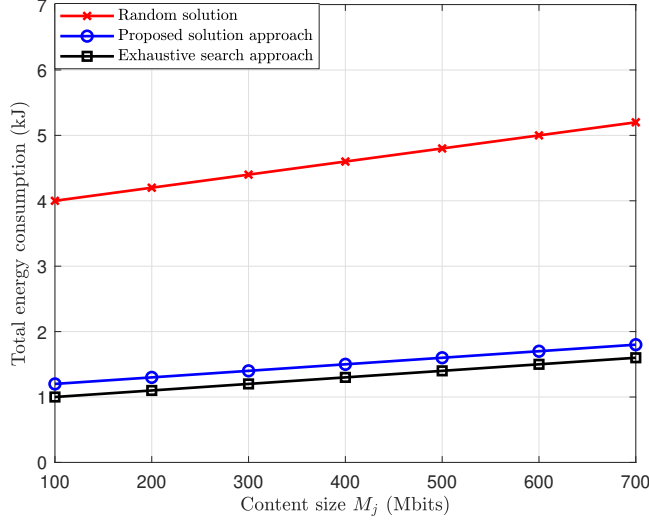


Fig. 3. Total energy consumption versus the content size with $N_c = 3$, $N_s = 2$, $N_m = 2$, and $U = 3$.

UAVs are deployed, each UAV is placed above a randomly selected user, each user is associated with the nearest UAV, all the sensing users are active, and the transmit power and computing resources are equally allocated to the corresponding users. (II) Proposed solution approach: which represents the performance of the graph-based solution in Algorithm 3. (III) Exhaustive search approach: in which all the possible user-UAV association and the sensing user activation are examined, while the transmission power and computing resources are obtained using Algorithm 1 and Algorithm 2, respectively. It can be noticed that the proposed solution approach remarkably reduces the energy consumption in comparison with the random solution. On the other hand, the proposed approach provides close to the optimum solution obtained using the exhaustive search.

Figure 4 provides insight into the effect of the number of users and the degree of correlation ρ of the gathered data on the energy expenditure of the proposed algorithm. It can be noticed that the energy expenditure increases with the number of users. It can also be noticed that the energy expenditure decreases as the degree of correlation increases. This can be attributed to the fact that as the degree of correlation increases, the data of the users becomes more correlated, and thus, fewer sensing users will meet the sensing tenant requirement. Furthermore, this behaviour indicates that the proposed solution approach activates an adequate number of data-gathering users, and as the degree of correlation

increases, fewer users are activated.

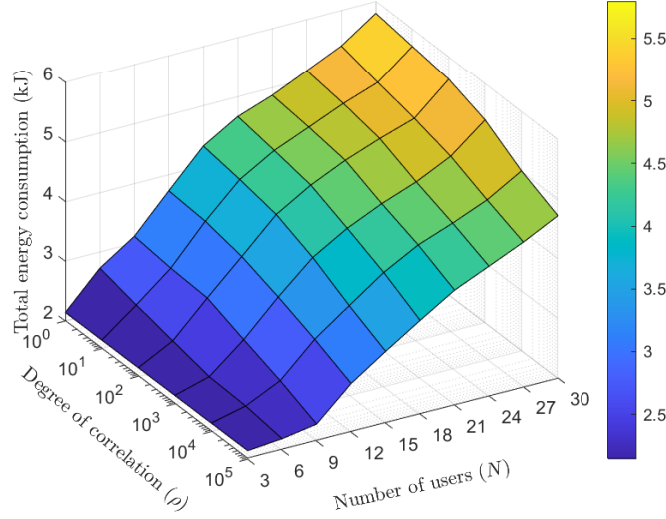


Fig. 4. Total energy consumption versus the degree of correlation ρ and number of users N .

To illustrate the effect of the number of the available UAVs and the computing speed, Fig. 5 illustrates the energy expenditure performance obtained using the proposed algorithm. It can be seen that the energy expenditure decreases as more UAVs are made available, and the floor behaviour occurs as the number of available UAVs increases. Such behaviour indicates that the number of deployed UAVs is optimized, and the proposed solution approach avoids deploying redundant UAVs, which otherwise lead to higher energy consumption. It can also be noticed that the energy expenditure increases as the computing speed decreases, which can be attributed to the fact that a slower computing speed at the UAV yields a longer hovering time and more energy consumption.

To study the effect of the number of deployed UAVs and their content storage capacity, Fig. 6 shows the energy consumption versus the number of deployed UAVs. This figure illustrates a heuristic placement solution, in which the users are clustered using a K -means clustering technique, and K UAVs are deployed each serving a cluster of users. Three UAV content storage capacities are illustrated, such that $\Gamma = 25\%$, $\Gamma = 50\%$, and $\Gamma = 100\%$ imply that each UAV stores one-fourth, half, and all the contents, respectively. It is worth mentioning that to guarantee that all contents are available to users, at least four and two UAVs are deployed for $\Gamma = 25\%$ and $\Gamma = 50\%$, respectively. It can be noticed that

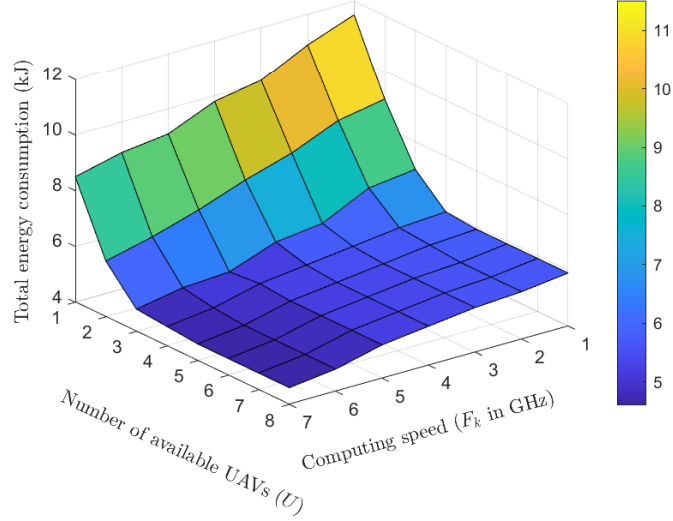


Fig. 5. Total energy consumption versus the degree of correlation ρ and number of users N .

as the storage capacity of the UAVs increases, less UAVs are required to be deployed and the corresponding energy consumption is less. This is a result of the fact that increasing the UAV storage capacity enables it to serve more users. Consequently, fewer UAVs are deployed, and the energy consumed by the deployed UAVs is less than that of deploying a higher number of UAVs with redundant stored content. It can be also noticed that deploying more UAVs increases the energy consumption as each UAV consumes traveling energy and serves less users.

The effect of the minimum required information by the data gathering tenant I is illustrated in Fig. 7. The considered range of I lies between 0 (which represents the extreme case, in which the tenant is not interested in gathering any information) and H (which means the tenant is interested in gathering all the available information). It can be seen that the energy consumption increases with I , which can be attributed to the fact that as I increases, more data-gathering users need to be activated and served by the UAVs. Furthermore, the figure depicts different values of the path loss exponent β . As the value of β increases, more energy is consumed. This is a result of the fact that increasing the value of the path loss exponent β reduces the achievable data rate, which leads to higher hovering time for the UAVs, and thus, increases the energy consumption. It is worth mentioning that changing the value of the Rician factor F within a reasonable range does not noticeably

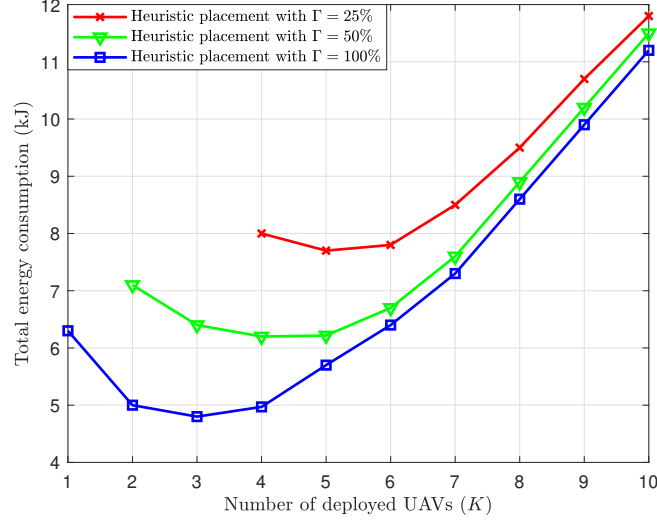


Fig. 6. Total energy consumption versus the number of deployed UAVs K with different UAV storage capacity.

affect the total energy consumption.

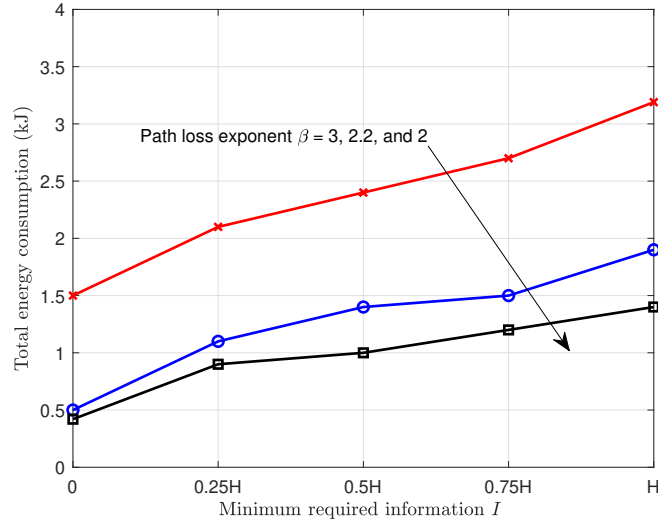


Fig. 7. Total energy consumption versus the minimum required information by the data gathering tenant I for different values of the path loss exponent β .

VI. Conclusion

This paper has introduced an energy-efficient network-slicing framework to deliver content and to gather information to/from the users as well as to provide MEC services. The MEC

tenant serves its users, the content delivery tenant mandates that each of its users receives the required content, and the sensing tenant needs to gather a sufficient amount of uncorrelated information. An energy consumption minimization optimization has been formulated to meet the tenants' requirements. The spatial correlation among the sensing users has been considered to activate the necessary subset of sensing users. A graph-based solution with the Lagrange approach has been developed. Simulation results have shown that the considered network-slicing framework significantly reduces the total energy consumption. This energy preservation is achieved by deploying a sufficient number of UAVs and optimally placing them, activating an adequate number of data-gathering users, efficiently associating the users with the deployed UAVs, and optimally allocating the transmit power and computing resources. Results also illustrated that the proposed solution provides performance close to the optimum one, with remarkably less computation complexity.

References

- [1] W. Rafique, J. Rani Barai, A. O. Fapojuwo, and D. Krishnamurthy, "A survey on beyond 5G network slicing for smart cities applications," *IEEE Commun. Surv. Tutor.*, vol. 27, no. 1, pp. 595–628, Feb. 2025.
- [2] S. Zhao, G. Qi, T. He, J. Chen, Z. Liu, and K. Wei, "A survey of sparse mobile crowdsensing: Developments and opportunities," *IEEE Open J. Comput. Soc.*, vol. 3, pp. 73–85, May 2022.
- [3] A. A. Al-habob, O. A. Dobre, and H. Vincent Poor, "Energy-efficient spatially-correlated data aggregation using unmanned aerial vehicles," in *Proc. IEEE 31st Annual International Symposium on Personal, Indoor and Mobile Radio Communications*, 2020, pp. 1–6.
- [4] A. A. Al-Habob, O. A. Dobre, and H. V. Poor, "Role assignment for spatially-correlated data aggregation using multi-sink internet of underwater things," *IEEE Trans. Green Commun. Netw.*, vol. 5, no. 3, pp. 1570–1579, Apr. 2021.
- [5] —, "Age- and correlation-aware information gathering," *IEEE Wireless Commun. Lett.*, vol. 11, no. 2, pp. 273–277, Nov. 2022.
- [6] A. A. Al-Habob, Y. N. Shnaiwer, S. Sorour, N. Aboutorab, and P. Sadeghi, "Multi-client file download time reduction from cloud/fog storage servers," *IEEE Trans. Mobile Comput.*, vol. 17, no. 8, pp. 1924–1937, Dec. 2018.
- [7] A. A. Al-Habob, O. A. Dobre, S. Muhaidat, and H. Vincent Poor, "Energy-efficient data dissemination using a UAV: An ant colony approach," *IEEE Wireless Commun. Lett.*, vol. 10, no. 1, pp. 16–20, Aug. 2021.
- [8] A. A. Al-Habob, O. A. Dobre, S. Muhaidat, and H. V. Poor, "Energy-efficient information placement and delivery using UAVs," *IEEE Internet Things J.*, vol. 10, no. 1, pp. 357–366, Jan. 2023.
- [9] B. Mao, Y. Liu, Z. Wei, H. Guo, Y. Xun, J. Wang, J. Liu, and N. Kato, "A blockchain-enabled cold start aggregation scheme for federated reinforcement learning-based task offloading in zero trust LEO satellite networks," *EEE J. Sel. Areas Commun.*, vol. 43, no. 6, pp. 2172–2182, Jun. 2025.
- [10] A. A. Al-habob, J. Lin, O. A. Dobre, and Y. Jing, "Min-max latency minimization for energy-constrained multi-UAV mobile edge computing," *IEEE Trans. Netw. Sci. Eng.*, vol. 11, no. 5, pp. 4577–4590, 2024.

- [11] Z. Xiao, L. Zhu, Y. Liu, P. Yi, R. Zhang, X.-G. Xia, and R. Schober, "A survey on millimeter-wave beamforming enabled UAV communications and networking," *IEEE Commun. Surv. Tutor.*, vol. 24, no. 1, pp. 557–610, First quarter 2022.
- [12] Y. Kawamoto, M. Takahashi, S. Verma, N. Kato, H. Tsuji, and A. Miura, "Traffic-prediction-based dynamic resource control strategy in HAPS-mounted MEC-assisted satellite communication systems," *IEEE Internet Things J.*, vol. 11, no. 8, pp. 13 824–13 836, Apr. 2024.
- [13] C. You and R. Zhang, "3D trajectory optimization in rician fading for UAV-enabled data harvesting," *IEEE Trans. Wireless Commun.*, vol. 18, no. 6, pp. 3192–3207, Apr. 2019.
- [14] C. De Alwis, P. Porambage, K. Dev, T. R. Gadekallu, and M. Liyanage, "A survey on network slicing security: Attacks, challenges, solutions and research directions," *IEEE Commun. Surv. Tutor.*, vol. 26, no. 1, pp. 534–570, First quarter 2024.
- [15] F. Wei, G. Feng, S. Qin, Y. Peng, and Y. Liu, "Hierarchical network slicing for UAV-assisted wireless networks with deployment optimization," *EEE J. Sel. Areas Commun.*, vol. 42, no. 12, pp. 3705–3718, Dec. 2024.
- [16] F. Wei, Y. Wang, G. Feng, and S. Qin, "Network slicing-enabled computation offloading in satellite-terrestrial edge computing networks: A bi-level game approach," *IEEE Internet Things J.*, vol. Early Access, pp. 1–16, 2025.
- [17] N. Xiong, W. Zhong, Y. Chen, D. He, Y. Li, L. Chen, and W. Liang, "MCDS: An effective multi-UAV collaborative decision-making system in mobile-edge computing networks," *IEEE Internet Things J.*, vol. 12, no. 15, pp. 29 354–29 372, Aug. 2025.
- [18] B. Xiao, Z. Yao, L. Zhang, B. Zhang, and C. Li, "An efficient online task offloading algorithm for bilevel UAV-enabled mobile edge computing," *IEEE Internet Things J.*, vol. Early Access, pp. 1–1, Jul. 2025.
- [19] H. H. Esmat, X. Liu, B. Lorenzo, and J. Liu, "Outage-aware multi-domain network slicing for satellite-airborne-terrestrial networks with multiple configurations," *IEEE Trans. Wireless Commun.*, vol. Early Access, pp. 1–1, Jul. 2025.
- [20] G. Faraci, C. Grasso, and G. Schembra, "Design of a 5G network slice extension with MEC UAVs managed with reinforcement learning," *EEE J. Sel. Areas Commun.*, vol. 38, no. 10, pp. 2356–2371, Oct. 2020.
- [21] S. Patten, B. Krishnamachari, and R. Govindan, "The impact of spatial correlation on routing with compression in wireless sensor networks," *ACM Trans. Sensor Netw.*, vol. 4, no. 4, pp. 1–33, Aug. 2008.
- [22] Y. Zeng, J. Xu, and R. Zhang, "Energy minimization for wireless communication with rotary-wing UAV," *IEEE Trans. Wireless Commun.*, vol. 18, no. 4, pp. 2329–2345, Mar. 2019.
- [23] M. B. Ghorbel, D. Rodríguez-Duarte, H. Ghazzai, M. J. Hossain, and H. Menouar, "Joint position and travel path optimization for energy efficient wireless data gathering using unmanned aerial vehicles," *IEEE Trans. Veh. Technol.*, vol. 68, no. 3, pp. 2165–2175, Mar. 2019.
- [24] Y. Wang, M. Sheng, X. Wang, L. Wang, and J. Li, "Mobile-edge computing: Partial computation offloading using dynamic voltage scaling," *IEEE Trans. Commun.*, vol. 64, no. 10, pp. 4268–4282, Aug. 2016.
- [25] S. Boyd and L. Vandenberghe, *Convex Optimization*. Cambridge university press, 2004.
- [26] M. Alzenad, A. El-Keyi, F. Lagum, and H. Yanikomeroglu, "3-D placement of an unmanned aerial vehicle base station (UAV-BS) for energy-efficient maximal coverage," *IEEE Wireless Commun. Lett.*, vol. 6, no. 4, pp. 434–437, Aug. 2017.